

# Efficient simulation of relativistic fermions via vertex models

Urs Wenger

*Institute for Theoretical Physics, University of Bern, Sidlerstrasse 5, CH-3012 Bern, Switzerland*  
(Dated: December 18, 2008)

We have developed an efficient simulation algorithm for strongly interacting relativistic fermions in two-dimensional field theories based on a formulation as a loop gas. The loop models describing the dynamics of the fermions can be mapped to statistical vertex models and our proposal is in fact an efficient simulation algorithm for generic vertex models in arbitrary dimensions. The algorithm essentially eliminates critical slowing down by sampling two-point correlation functions and it allows simulations directly in the massless limit. Moreover, it generates loop configurations with fluctuating topological boundary conditions enabling to simulate fermions with arbitrary periodic or anti-periodic boundary conditions. As illustrative examples, the algorithm is applied to the Gross-Neveu model and to the Schwinger model in the strong coupling limit.

PACS numbers: 02.70.-c, 05.50.+q, 11.10.Kk, 11.15.Ha

Simulating strongly interacting fermions, like in Quantum Chromodynamics (QCD) or in Nambu–Jona–Lasinio models, is considered to be rather difficult and continues to be a challenge. Contrary to common lore, this is not directly due to the fact that the fermionic degrees of freedom are Grassmannian variables, but rather due to the non-locality of the determinant which is obtained upon integrating out the fermionic fields. Moreover, simulations of fermions are usually hampered by critical slowing down towards the chiral limit where the fermions become massless and the correlation length of the fermionic two-point function diverges. The established standard method to perform such calculations on the lattice is to use the Hybrid Monte-Carlo algorithm [1] which deals with the non-locality of the determinant by rewriting it as an integral over bosonic “pseudo-fermion” fields. The algorithm then requires to deal with the inverse of the fermion Dirac operator, however, the operator becomes ill-conditioned towards the massless limit and the simulations slow down dramatically. In this letter we propose a novel approach which circumvents the above mentioned problems. It is based on a (high-temperature) expansion of the fermion actions which reformulates the fermionic systems as  $q$ -state vertex models, i.e., statistical closed loop models. In particular, the method is directly applicable to the Gross-Neveu (GN) model and to the Schwinger model in the strong coupling limit. These models can be shown to be equivalent to specific vertex models [2, 3, 4, 5] and our simulation method, based on a proposal by Prokof’ev and Svistunov [6], is effectively a very efficient updating algorithm for generic vertex models (in arbitrary dimensions). In fact, the algorithm essentially eliminates critical slowing down and is able to simulate the fermionic systems at the critical point and directly in the massless limit.

We start with illustrating the reformulation in terms of closed loops in the GN model. The model is most naturally formulated by employing Majorana fermions [7, 8]. Here we are using Wilson’s Euclidean lattice discretisa-

tion for which the action density of the model is

$$\mathcal{L}_{\text{GN}} = \frac{1}{2} \xi^T \mathcal{C} (\gamma_\mu \tilde{\partial}_\mu - \frac{1}{2} \partial^* \partial + m) \xi - \frac{g^2}{4} (\xi^T \mathcal{C} \xi)^2, \quad (1)$$

where  $\xi$  is a real, two component Grassmann field describing a Majorana fermion with mass  $m$ ,  $\mathcal{C} = -\mathcal{C}^T$  is the charge conjugation matrix, and  $\partial, \partial^*, \tilde{\partial}$  denote the forward, backward and symmetric lattice derivative, respectively. The Wilson term  $\frac{1}{2} \partial^* \partial$ , responsible for removing the fermion doublers, explicitly breaks the discrete chiral symmetry  $\xi \rightarrow \gamma_5 \xi, \xi^T \mathcal{C} \rightarrow \xi^T \mathcal{C} \gamma_5$  and requires a fine tuning of  $m \rightarrow m_c$  towards the continuum limit in order to restore the symmetry. A pair  $\xi_1, \xi_2$  of Majorana fermions may be considered as one Dirac fermion using the identification  $\psi = \frac{1}{\sqrt{2}}(\xi_1 + i\xi_2)$ ,  $\bar{\psi} = \frac{1}{\sqrt{2}}(\xi_1^T - i\xi_2^T)\mathcal{C}$  and the corresponding GN model with  $N$  Dirac fermions has an  $O(2N)$  flavour symmetry. At  $g = 0$ , integrating out the Grassmann variables yields the partition function in terms of the Pfaffian

$$Z_{\text{GN}} = \text{Pf} \left[ \mathcal{C} (\gamma_\mu \tilde{\partial}_\mu + m - \frac{1}{2} \partial^* \partial) \right]^{2N}. \quad (2)$$

For  $g \neq 0$  one usually performs a Hubbard-Stratonovich transformation and introduces a scalar field  $\sigma$  conjugate to  $\xi^T \mathcal{C} \xi$  which yields the new fermionic action

$$S = \frac{1}{2} \sum_x \xi^T(x) \mathcal{C} (2 + m + \sigma(x)) \xi(x) - \sum_{x,\mu} \xi^T(x) \mathcal{C} \frac{1 - \gamma_\mu}{2} \xi(x + \hat{\mu}), \quad (3)$$

together with an additional Gaussian Boltzmann factor  $\exp\{-1/(2g^2) \sum_x \sigma(x)^2\}$  for the scalar field.

In order to reformulate the model in terms of closed loops (or equivalently dimers and monomers) we follow the recent derivation of Wolff [7] (see [4, 5] for alternative, but more complicated derivations). One simply expands the Boltzmann factor for the fermionic fields and makes

use of the nil-potency of the Grassmann variables upon integration. Introducing  $\varphi(x) = 2 + m + \sigma(x)$  and the projectors  $P(\pm\mu) = (1 \mp \gamma_\mu)/2$  we can write the fermionic part of the GN path integral (up to an overall sign) as

$$\int \mathcal{D}\xi \prod_x (\varphi(x) \xi^T(x) \mathcal{C} \xi(x))^{m(x)} \prod_{x,\mu} (\xi^T(x) \mathcal{C} P(\mu) \xi(x + \hat{\mu}))^{b_\mu(x)} \quad (4)$$

where  $m(x) = 0, 1$  and  $b_\mu(x) = 0, 1$  are the monomer and bond (or dimer) occupation numbers, respectively. Integration over the fermion fields yields the constraint that at each site  $m(x) + \frac{1}{2} \sum_\mu b_\mu(x) = 1$ . Here the sum runs over positive and negative directions and  $b_{-\mu}(x) = b_\mu(x - \hat{\mu})$ . The constraint ensures that only closed and non-intersecting loops of occupied bonds contribute to the partition function and also accounts for the fact that the loops are non-backtracking, a consequence of the orthogonal projectors  $P(\pm\mu)$ . The weight  $\omega(\ell)$  of each loop  $\ell$  can be calculated analytically [9] and yields  $|\omega(\ell)| = 2^{-n_c/2}$  where  $n_c$  is the number of corners along the loop. The sign of  $\omega$  will generically depend on the geometrical shape of the loop [9] prohibiting a straightforward probabilistic interpretation of the loop weights in dimensions  $d > 2$ .

In two dimensions, however, the sign of the loop only depends on the topology of the loop, as recently clarified by Wolff [7], and is determined by the fermionic boundary conditions. It is therefore useful to classify all loop configurations into the four equivalence classes  $\mathcal{L}_{00}, \mathcal{L}_{10}, \mathcal{L}_{01}, \mathcal{L}_{11}$  where the index denotes the total winding (modulo two) of the loops in the two directions. The weights of all configurations in  $\mathcal{L}_{10}$  and  $\mathcal{L}_{11}$  for example will pick up an overall minus sign if we change the fermionic boundary condition in the first direction from periodic to antiperiodic, while the weights of the configurations in  $\mathcal{L}_{00}$  and  $\mathcal{L}_{01}$  remain unaffected. As a consequence, if we sum over all the topological equivalence classes with positive weights, i.e.,  $Z \equiv Z_{\mathcal{L}_{00}} + Z_{\mathcal{L}_{10}} + Z_{\mathcal{L}_{01}} + Z_{\mathcal{L}_{11}}$  we effectively describe a system with unspecified fermionic boundary conditions. Vice versa, the partition function  $Z_\xi^{10} \equiv Z_{\mathcal{L}_{00}} + Z_{\mathcal{L}_{10}} - Z_{\mathcal{L}_{01}} - Z_{\mathcal{L}_{11}}$ , e.g., describes a system with fermionic b.c. antiperiodic in the first and periodic in the second direction.

Before describing our method to simulate the loop formulation of the GN model, essentially generating closed loop configurations according to their loop weight, it is useful to point out the equivalence to the 8-vertex model [10, 11]. The model is formulated in terms of the eight vertex configurations shown in the top row of Fig. 1 with weights  $\omega_i, i = 1, \dots, 8$ . The partition function is then defined as the sum over all possible tilings of the square lattice with the eight vertices such that only closed (but

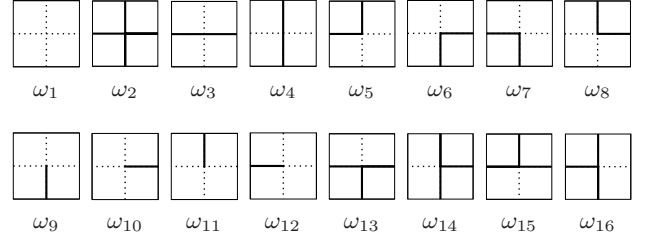


FIG. 1: The vertex configurations and weights of the eight-vertex model (top row) and the extended model (bottom row).

possibly intersecting) paths occur. To be precise, one has

$$Z_{8\text{-vertex}} = \sum_{\text{CP}} \prod_x \omega_i(x). \quad (5)$$

where the sum is over all closed path configurations (CP) and the weight of each configuration is given by the product of all vertex weights in the configuration. For the GN model we have the following weights

$$\begin{aligned} \omega_1 &= \varphi(x), & \omega_3 &= \omega_4 = 1, \\ \omega_2 &= 0, & \omega_5 &= \omega_6 = \omega_7 = \omega_8 = \frac{1}{\sqrt{2}}, \end{aligned} \quad (6)$$

i.e. each corner contributes a factor  $1/\sqrt{2}$ , while crossings of two lines are forbidden ( $\omega_2 = 0$ ) and each empty site carries the monomer weight  $\omega_1 = \varphi(x)$ . From here it also becomes clear that for a single Majorana fermion the interaction term proportional to  $g$  is irrelevant. Since the partition function is now factorised into terms at each  $x$  we can integrate over the scalar field  $\sigma(x)$  at each site separately. However, since the integration measure is even in  $\sigma(x)$  the term linear in  $\sigma(x)$  will not survive and the monomer weight reduces to  $\omega_1 = 2 + m$ . This is how the free Majorana fermion is recovered after the Hubbard-Stratonovich transformation. If one considers two or more Majorana flavours which are coupled through the four-fermion interaction, the integration over  $\sigma(x)$  becomes non-trivial, but can still be done analytically [5] yielding 8-vertex models coupled to each other. It should be stressed, however, that from an algorithmic point of view the generic case with an arbitrarily varying field  $\sigma(x)$  is equally accessible and involves no complication whatsoever.

The fact that the GN model with a single Majorana fermion is effectively a free fermion system expresses itself also through the vertex weights fulfilling the free fermion condition [10, 12]  $\omega_1\omega_2 + \omega_3\omega_4 = \omega_5\omega_6 + \omega_7\omega_8$ . 8-vertex models fulfilling the free fermion condition as well as those in zero field [13, 14] are analytically solvable, in particular also the standard Ising model. We use this fact to our convenience and use the Majorana GN model as a benchmark which allows to compare the results of our algorithm with analytic results. Instances of the 8-vertex model for which no analytic solutions are known, but are accessible with our algorithm, include the Ising model

with additional next-to-nearest-neighbour and quartic interactions [13]. Another 8-vertex model with a fermionic interpretation is the one-flavour Schwinger model with Wilson fermions in the strong coupling limit [2, 15]. The vertex weights are given by

$$\begin{aligned} \omega_1 &= (m+2)^2, & \omega_3 &= \omega_4 = 1, \\ \omega_2 &= 0, & \omega_5 &= \omega_6 = \omega_7 = \omega_8 = \frac{1}{2}, \end{aligned} \quad (7)$$

where the monomer weight and the corner weights are squared due to the fact that we are dealing with a pair of Majorana fermions glued together [18].

Let us now turn to the description of the new method to efficiently simulate any vertex model in arbitrary dimensions with generic (positive) weights  $\omega_i$ , including the fermionic models discussed above. For illustrative purpose we restrict the discussion to the 8-vertex model. The method is an extension of the so-called worm algorithm by Prokof'ev and Svistunov [6]. The configuration space of closed loops is enlarged to contain also open strings. For the GN model such an open string with ends at  $x$  and  $y$  corresponds to the insertion of two Majorana fields at positions  $x$  and  $y$  which is simply the Majorana fermion propagator

$$G(x, y) = \int \mathcal{D}\xi e^{-S_{\text{GN}}} \xi(x)\xi(y)^T \mathcal{C}. \quad (8)$$

Similar interpretations of the open string can be obtained for other vertex models. The open string is now the basis for a Monte Carlo algorithm which samples directly the space of 2-point correlation functions instead of the standard configuration space. This is the reason why the algorithm is capable of beating critical slowing down as demonstrated below: at a critical point where the correlation length grows large, the configurations are updated equally well on all length scales up to a scale of the order of the correlation length.

In the vertex language the insertions correspond to the new vertex configurations depicted in the bottom row of Fig. 1. A configuration containing a single open string corresponds to a loop configuration with two instances of vertex 9-16 which are connected by a string. Note that vertices 13-16, while present in the generic extended vertex-model, do not have a physical interpretation in terms of fermionic fields since they are explicitly forbidden by Pauli's exclusion principle (fermionic lines are not allowed to intersect). Nevertheless they can also be included in the fermionic models, simply for algorithmic efficiency, and we do so in our implementation.

The algorithm now proceeds by locally updating the ends of the open string using a simple Metropolis or heat bath step according to the weights of the corresponding 2-point function. When one end is shifted from, say,  $x$  to one of its neighbouring points  $y$ , a dimer on the corresponding bond is destroyed or created depending on whether the bond is occupied or not. In the process, the

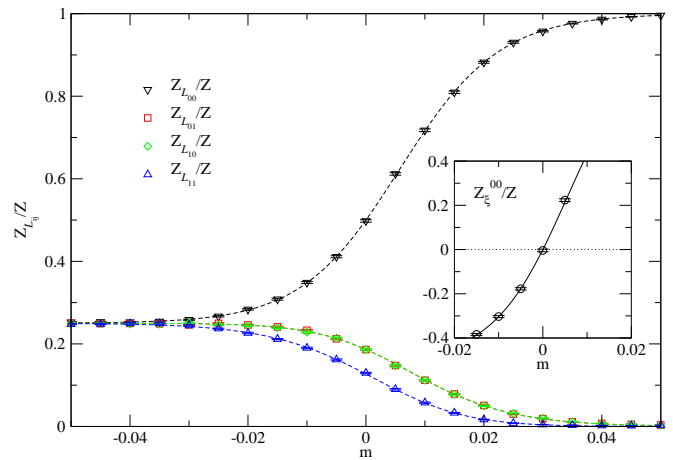


FIG. 2: Results for the ratios  $Z_{\mathcal{L}_{ij}}/Z$  with  $i, j = 0, 1$  for the Majorana GN model on a  $128^2$  lattice as a function of the bare mass  $m$ . Dashed lines are the exact results calculated from the Pfaffians. Note that the curves and the data for  $Z_{\mathcal{L}_{10}}/Z$  and  $Z_{\mathcal{L}_{01}}/Z$  lie on top of each other. The inset shows the partition function ratio  $Z_{\xi}^{00}/Z$  and illustrates how the zero mode at  $m = 0$  is reproduced.

two vertices at  $x$  and  $y$  are changed from  $v_x, v_y$  to  $v'_x, v'_y$  and the move is accepted with probability

$$P(x \rightarrow y) = \min \left[ 1, \frac{\omega_{v'_x} \omega_{v'_y}}{\omega_{v_x} \omega_{v_y}} \right] \quad (9)$$

in order to satisfy detailed balance. So a global update results from a sequence of local moves, and in this sense it is similar in spirit to the loop cluster update suggested in [16].

Whenever the two ends of the open string meet, a new closed loop is formed and the new configuration contributes to the original partition function  $Z$  in one of the classes  $\mathcal{L}_{00}, \mathcal{L}_{10}, \mathcal{L}_{01}, \mathcal{L}_{11}$ . In this way the overall normalisation is ensured, and expectation values can be calculated as usual. From here it also becomes clear that the algorithm switches between the topological sectors with ease: as the string evolves it can grow or shrink in any direction and wrap around the torus as many times as it likes. Effectively, the algorithm simulates a system with fluctuating topological boundary conditions.

In principle, the weight of the open string can be chosen arbitrarily, but the physical interpretation given by eq.(8) suggests to choose the weights  $\omega_9$  to  $\omega_{16}$  such that the open string configurations sample directly the 2-point correlation function. The open string configurations then provide an improved estimator for the 2-point correlation function [19]. During the simulation one simply updates a table for  $G(x, y)$  as the string endpoints move around and the expectation value is obtained by forming  $\langle G(x, y) \rangle_Z = G(x, y)/Z$ . For the fermionic models we also need to keep track of the Dirac structure associated with  $G(x, y)$ . This is most easily done by adding

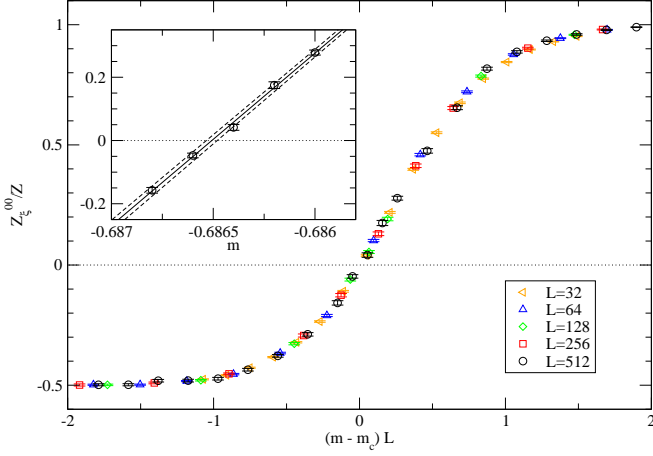


FIG. 3: Results for the ratio  $Z_{\xi}^{00}/Z$  in the Schwinger model at strong coupling for various system sizes. The inset shows the determination of the critical mass  $m_c = -0.686506(27)$  while the main plot shows the collapse from finite size scaling consistent with a second order phase transition in the universality class of the Ising model (with critical exponent  $\nu = 1$ ).

the product of the Dirac projectors along the string  $\ell$ , i.e.  $\prod_{\mu \in \ell} P(\mu)$ , as a contribution at each step. Care has to be taken when the open string winds an odd times around a boundary on which we want to impose antiperiodic boundary conditions for the fermions. In that case we need to account for an additional minus sign in the contribution to  $G(x, y)$ . For the fermionic models where vertices 13-16 have no physical meaning, the weights  $\omega_{13}$  to  $\omega_{16}$  can be tuned for algorithmic efficiency and do not follow any physically inspired rule. A good choice is to use the geometric mean of the weights  $\omega_i$  of those vertices that can be reached in one further update step, e.g.  $\omega_{13} = (\omega_4 \omega_6 \omega_7)^{1/3}$ . Finally, let us emphasise again that the algorithm described here is applicable to any vertex model, also in higher dimensions, as long as the weights are positive definite in well defined configuration classes.

We have performed extensive tests of our algorithm by comparing to exact results known from Pfaffians (for the Majorana GN model) or from explicit calculations on small lattices. Simple observables are linear combinations of partition functions and ratios thereof, e.g.  $Z_{\mathcal{L}_{ij}}/Z$  with  $i, j = 0, 1$ . In Fig. 2 we show the results for the ratios  $Z_{\mathcal{L}_{ij}}/Z$  in the Majorana GN model on a  $128^2$  lattice as a function of the bare mass  $m$ . Dashed lines are the exact results calculated from the Pfaffians. Note that all partition function ratios are obtained in the same simulation. In the inset we also show the ratio  $Z_{\xi}^{00}/Z$  where  $Z_{\xi}^{00} \equiv Z_{\mathcal{L}_{00}} - Z_{\mathcal{L}_{01}} - Z_{\mathcal{L}_{10}} - Z_{\mathcal{L}_{11}}$  is the partition function with fermionic b.c. periodic in space and time direction. In that situation the Majorana Dirac operator has a zero mode at  $m = 0$  (and at  $m = -2$ ) and the system is critical. The inset in Fig. 2 illustrates that the algo-

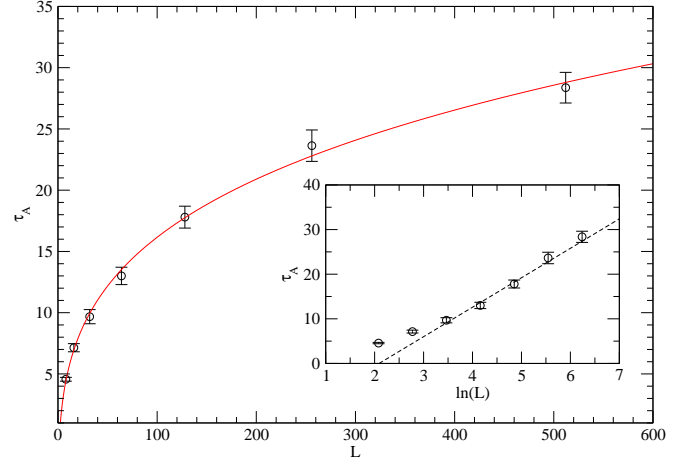


FIG. 4: Integrated autocorrelation time  $\tau_A$  of the energy for the Schwinger model in the strong coupling limit as a function of the system size  $L$  at the critical point  $m = m_c$ . The line is a fit  $\tau_A \propto L^z$  yielding  $z = 0.25(2)$ . The inset shows the logarithmic dependence  $-18(3) + 7.5(6) \ln(L)$  from fitting to  $L \geq 64$ .

rithm can reproduce this zero mode without problems and that we can in fact simulate directly at the critical point. Conversely, we can use  $Z_{\xi}^{00}/Z = 0$  as a definition of the critical point  $m = m_c$ . In Fig. 3 we show our results for  $Z_{\xi}^{00}/Z$  as a function of the bare mass  $m$  in the Schwinger model in the strong coupling limit for various volumes. The critical point can be determined accurately with very little computational effort and we obtain  $m_c = -0.686506(27)$  (cf. inset in Fig. 3) from our simulations on the largest lattice with  $L = 512$ . Further improvement could be achieved by employing standard reweighting techniques as done in [17] where they obtained  $m_c = -0.6859(4)$ . These calculations indicated a second order phase transition in the universality class of the Ising model (with critical exponent  $\nu \simeq 1$ ). Our results in Fig. 3 now confirm this by demonstrating that the partition function ratios  $Z_{\xi}^{00}/Z$  as a function of the rescaled mass  $(m - m_c)L^\nu$  with  $\nu = 1$  beautifully collapse onto a universal scaling curve.

The efficiency of the algorithm and the fact that critical slowing down is essentially absent is demonstrated in Fig. 4 where we show the integrated autocorrelation time  $\tau_A$  of the energy as a function of the linear system size  $L$  at the critical point  $m = m_c$ . (Similar plots can be obtained for the Majorana GN model.) The functional dependence on  $L$  can be well fitted ( $\chi^2/\text{dof} = 1.28$ ) by  $\tau_A \propto L^z$  all the way down to our smallest system size  $L = 8$ . We obtain  $z = 0.25(2)$  which is consistent with just using the largest two system sizes. It is an amazing result that our local Metropolis-type update appears to have a dynamical critical exponent close to zero. The autocorrelation time may also depend logarithmically on  $L$  and a fit to  $L \geq 64$  yields  $-13.8(1.9) + 6.6(4) \ln(L)$  with

$\chi^2/\text{dof} = 1.00$ .

In conclusion, we have presented a new type of algorithm for generic vertex models. It relies on sampling directly 2-point correlation functions and essentially eliminates critical slowing down. We have successfully tested our algorithm on the Majorana GN model and on the Schwinger model in the strong coupling limit and found remarkably small dynamical critical exponents. The algorithm definitely opens the way to simulate efficiently generic vertex models (with positive weights) in arbitrary dimensions, in particular the GN model with any number of flavours, the Thirring model, the Schwinger model in the strong coupling limit (in arbitrary dimensions), as well as fermionic models with Yukawa-type scalar interactions, all with Wilson fermions.

I would like to thank Philippe de Forcrand and Michael Fromm for useful and sometimes crucial discussions. This work is supported by SNF grant PP002-119015.

- 
- [1] S. Duane, A. D. Kennedy, B. J. Pendleton, and D. Roweth, Phys. Lett. **B195**, 216 (1987).
  - [2] M. Salmhofer, Nucl. Phys. **B362**, 641 (1991).
  - [3] K. Scharnhorst, Nucl. Phys. **B479**, 727 (1996), hep-lat/9604024.

- [4] K. Scharnhorst, Nucl. Phys. **B503**, 479 (1997), hep-lat/9611005.
- [5] C. Gattringer, Nucl. Phys. **B543**, 533 (1999), hep-lat/9811014.
- [6] N. Prokof'ev and B. Svistunov, Phys. Rev. Lett. **87**, 160601 (2001).
- [7] U. Wolff, Nucl. Phys. **B789**, 258 (2008), 0707.2872.
- [8] C. Itzykson and J. M. Drouffe, *Statistical Field Theory. Vol. 2* (Univ. Pr., Cambridge, 1989).
- [9] I. O. Stamatescu, Phys. Rev. **D25**, 1130 (1982).
- [10] C. Fan and F. Y. Wu, Phys. Rev. **B2**, 723 (1970).
- [11] B. Sutherland, J. Math. Phys. **11**, 3183 (1970).
- [12] C. Fan and F. Y. Wu, Phys. Rev. **179**, 560 (1969).
- [13] R. J. Baxter, *Exactly solved models in statistical mechanics* (Academic Press, London, 1982).
- [14] R. J. Baxter, Phys. Rev. Lett. **26**, 832 (1971).
- [15] C. Gattringer, Nucl. Phys. **B559**, 539 (1999), hep-lat/9903021.
- [16] H. G. Evertz, G. Lana, and M. Marcu, Phys. Rev. Lett. **70**, 875 (1993), cond-mat/9211006.
- [17] H. Gausterer and C. B. Lang, Nucl. Phys. **B455**, 785 (1995), hep-lat/9506028.
- [18] One can in fact derive these weights also for  $d > 2$  and show that all loop contributions are positive, hence allowing simulations of the Schwinger model in the strong coupling limit in arbitrary dimensions.
- [19] Note that one can also sample  $(2n)$ -point correlation functions.